Breakdown voltage enhancement in GaN channel and AlGaN channel HEMTs using large gate metal height*

Zhong-Xu Wang(王中旭)[1], Lin Du(杜林)[2], Jun-Wei Liu(刘俊伟)[1], Ying Wang(王颖)[3], Yun Jiang(江芸)[2], Si-Wei Ji(季思蔚)[2], Shi-Wei Dong(董士伟)[3], Wei-Wei Chen(陈伟伟)[3], Xiao-Hong Tan(谭骁洪)[4], Jin-Long Li(李金龙)[4], Xiao-Jun Li(李小军)[3], Sheng-Lei Zhao(赵胜雷)[1,†], Jin-Cheng Zhang(张进成)[1,‡], and Yue Hao(郝跃)[1]

[1] Key Laboratory for Wide Band-Gap Semiconductor Materials and Devices, School of Microelectronics, Xidian University, Xi'an 710071, China
[2] Shanghai Precision Metrology and Testing Research Institute, Shanghai 201109, China
[3] China Academy of Space Technology (Xi'an), Xi'an 710000, China
[4] Sichuan Institute of Solid-State Circuits, CETC, Chongqing 400060, China

(Received 4 November 2019; revised manuscript received 5 December 2019; accepted manuscript online 9 December 2019)

A large gate metal height technique is proposed to enhance breakdown voltage in GaN channel and AlGaN channel high-electron-mobility-transistors (HEMTs). For GaN channel HEMTs with gate–drain spacing L_{GD} = 2.5 μm, the breakdown voltage V_{BR} increases from 518 V to 582 V by increasing gate metal height h from 0.2 μm to 0.4 μm. For GaN channel HEMTs with L_{GD} = 7 μm, V_{BR} increases from 953 V to 1310 V by increasing h from 0.8 μm to 1.6 μm. The breakdown voltage enhancement results from the increase of the gate sidewall capacitance and depletion region extension. For $Al_{0.4}Ga_{0.6}N$ channel HEMT with L_{GD} = 7 μm, V_{BR} increases from 1535 V to 1763 V by increasing h from 0.8 μm to 1.6 μm, resulting in a high average breakdown electric field of 2.51 MV/cm. Simulation and analysis indicate that the high gate metal height is an effective method to enhance breakdown voltage in GaN-based HEMTs, and this method can be utilized in all the lateral semiconductor devices.

Keywords: GaN channel HEMTs, AlGaN channel HEMTs, breakdown voltage, gate metal height

PACS: 73.40.Kp, 73.61.Ey, 78.30.Fs **DOI:** 10.1088/1674-1056/ab5fb9

1. Introduction

GaN-based high-electron-mobility-transistors (HEMTs) have been promising candidates for high voltage and high frequency applications due to their superior material and device characteristics.[1–3] The critical electric fields for GaN and AlN are 3.3 MV/cm and 12 MV/cm, respectively, and the AlGaN material is a kind of ultra-wide bandgap (UWBG) semiconductor with better breakdown characteristics compared with the GaN material. The off-state breakdown voltage (BV) is one of the most important parameters for GaN-based HEMTs, and numerous studies concentrate on improving the breakdown characteristics.[4–6] For GaN channel HEMTs, a record high breakdown voltage of 3000 V has been achieved in InAlN/GaN MOSHEMT with gate–drain spacing of 30 μm.[7] In comparison, a BV of 1650 V has been obtained in AlGaN channel HEMT with gate–drain spacing of 10 μm.[8,9] In order to improve BV, several methods were employed, including source field plate (FP), gate FP, AlGaN back barrier, and high-k passivation layer.[10–12] However, the gate–drain average breakdown electric field E_{BR} values are much lower than the theoretical limitation ones for GaN channel and AlGaN channel HEMTs. For GaN-based HEMTs, it is difficult to achieve BV of 1 kV and E_{BR} of 2 MV/cm simultaneously. It is essential to further improve the BV and E_{BR} of GaN-based HEMTs.

In this paper, a simple method, large gate metal height, is proposed to enhance BV in GaN channel and AlGaN channel HEMTs. By using this method, breakdown voltage V_{BR} of 582 V and E_{BR} of 2.33 MV/cm have been achieved for GaN channel HEMTs with gate–drain spacing $L_{GD} = 2.5$ μm. For AlGaN channel HEMTs with $L_{GD} = 7$ μm, V_{BR} and E_{BR} can be improved to 1736 V and 2.51 MV/cm, respectively.

2. Device structure and simulation model

The GaN and AlGaN channel HEMTs structure adopted in this paper is shown in Fig. 1. The devices are simulated by using Silvaco-ATLAS software. For the fabricated GaN-based HEMTs, the drain and source metals should penetrate into the GaN buffer layer and be connected to 2DEG directly by an annealing process to form ohmic contacts. The drain and source contacts are designed as shown in Fig. 1 to simulate this process, and the contact length $L_{con} = 0.5$ μm. The simulated HEMTs have a gate length $L_G = 1$ μm, a gate–source spacing $L_{GS} = 0.5$ μm, and a gate–drain spacing $L_{GD} = 2.5$–9 μm. For AlGaN channel HEMTs, the aluminum compositions for the AlGaN buffer and AlGaN barrier layers are 40% and 70%,

*Project supported by the National Key Science & Technology Special Project of China (Grant No. 2017ZX01001301), the National Key Research and Development Program of China (Grant No. 2016YFB0400100), and the National Natural Science Foundation of China (Grant Nos. 51777168 and 61801374).

†Corresponding author. E-mail: slzhao@xidian.edu.cn
‡Corresponding author. E-mail: jchzhang@xidian.edu.cn

respectively.

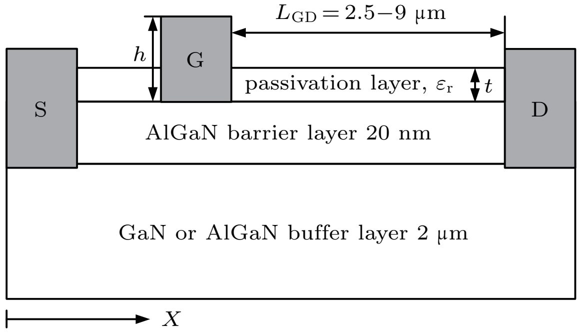

Fig. 1. Device structure of the GaN and AlGaN channel HEMTs.

The electron mobility in the AlGaN barrier layer is set to 600 $cm^2/V{\cdot}s$.[10] The GaN or AlGaN buffer layer consists of two parts, namely, 10-nm channel layer and 1.99-μm buffer layer. In the channel layer, the electrons belong to 2DEG and their mobility is set to 1500 $cm^2/V{\cdot}s$ according to the 2DEG mobility in previous studies.[13,14] The electron mobility in the buffer layer is set to 250 $cm^2/V{\cdot}s$, which is extracted from the GaN-based MOSFET.[15] In the buffer layer, we consider a shallow donor, a deep donor, and a deep acceptor.[12,16] The shallow donor is assumed to be ionized completely at room temperature, and its density is set to 1×10^{15} cm^{-3}. The energy level and density of the deep donor are $E_C - 0.5$ eV and 2×10^{17} cm^{-3}, respectively. The electron and hole capture cross sections for the deep donor are 1×10^{-13} cm^2 and 1×10^{-15} cm^2, respectively. The energy level and density of the deep acceptor are assumed to be $E_C - 2.85$ eV and 1×10^{17} cm^{-3}, respectively. The electron and hole capture cross sections for the deep acceptor are both set to 1×10^{-15} cm^2. The positive polarization charge is modeled as a positive fixed sheet charge with a density of 1×10^{13} cm^{-2} along the interface of the heterojunction. In this paper, surface states and gate tunneling model are not considered. The device breakdown is induced by the impact ionization. The impact ionization is modeled as $\alpha_0\exp(-E_C/E)$, where $\alpha_0 = 2.9\times10^8$ cm^{-1} and $E_C = 3.4\times10^7$ V/cm.[17]

3. Results and discussion

As shown in Fig. 2, AlGaN/GaN HEMTs with various relative permittivities ε_r are simulated. The gate height h and passivation layer thickness t are 0.2 μm and 0.1 μm, respectively. The breakdown voltage V_{BR} is defined as the drain voltage with the drain leakage current I_D reaching 1 mA/mm. V_{BR} increases with the increase of ε_r for one certain passivation layer thickness. For $\varepsilon_r = 3.9$ (SiO_2), the breakdown voltage is 99 V. In contrast, V_{BR} for the HEMT with $\varepsilon_r = 28$ ($LaLuO_3$) is 346 V, which is 2.5 times higher than that for the HEMT with $\varepsilon_r = 3.9$. When the passivation layer thickness increases to 0.5 μm, V_{BR} can be improved further to 518 V as shown in Fig. 3. The similar relationship between V_{BR} and ε_r and between V_{BR} and t is in agreement with the numerical calculation.[12] For a high ε_r or t, the electric field at the drain-side edge of the gate is weakened, and the applied voltage tends to drop uniformly.

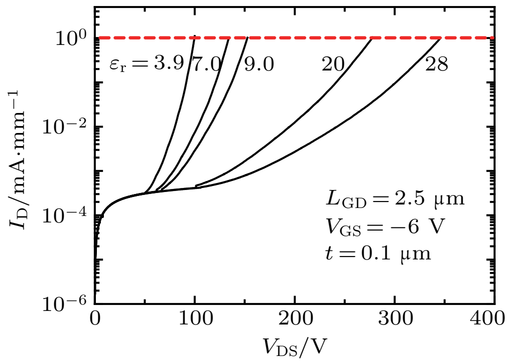

Fig. 2. Off-state I_D–V_{DS} curves for GaN channel HEMTs with various relative permittivities.

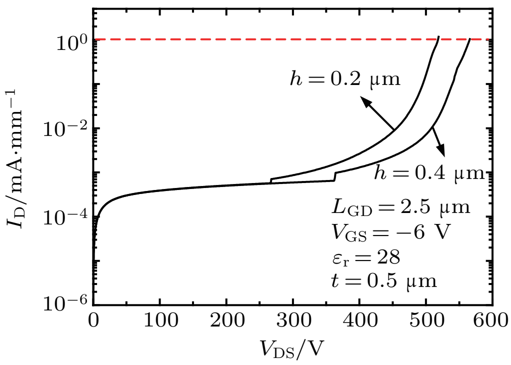

Fig. 3. Comparison of off-state I_D–V_{DS} curves for GaN channel HEMTs with $\varepsilon_r = 28$, $t = 0.5$ μm, and $h = 0.2$ μm or $h = 0.4$ μm.

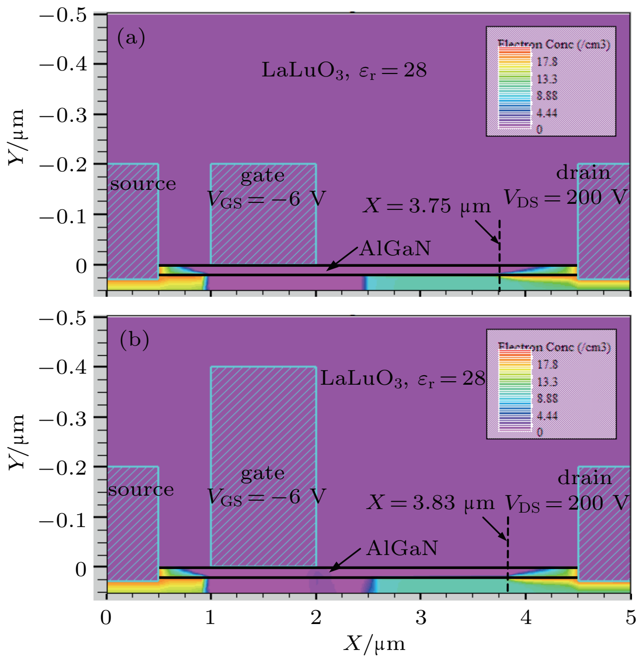

Fig. 4. Logarithmic electron concentration distribution in GaN channel HEMTs with $\varepsilon_r = 28$, $t = 0.5$ μm, $V_{DS} = 200$ V, and (a) $h = 0.2$ μm or (b) $h = 0.4$ μm.

The impact of gate metal thickness h on breakdown characteristics is shown in Fig. 3, the breakdown voltage V_{BR} increases from 518 V for $h = 0.2$ μm to 566 V for $h = 0.4$ μm. Figure 4 shows the electron concentration distribution in GaN channel HEMTs with $h = 0.2$ μm and $h = 0.4$ μm. The depletion region along the AlGaN/GaN interface can extend from $X = 3.75$ μm for $h = 0.2$ μm to $X = 3.83$ μm for $h = 0.4$ μm, indicating that a larger depletion region can be formed for a larger h. A larger h would increase the area of the drain-side wall of the gate and the gate sidewall capacitance. The increased depletion capacitance would enlarge the depletion region extension and improve the breakdown voltage. The relative permittivity of air is much lower than that of the passivation layer. In order to achieve a large gate sidewall capacitance, the passivation layer should be higher than the gate metal.

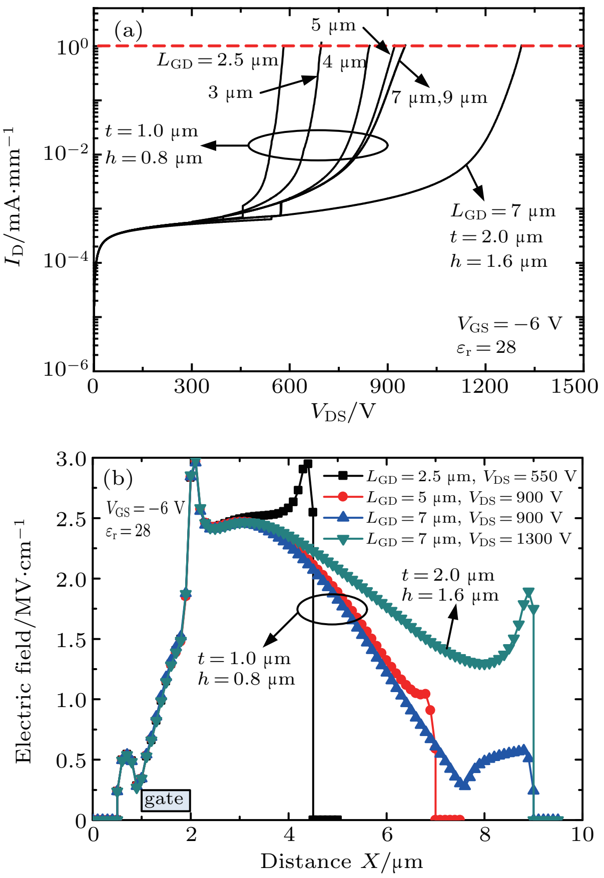

Fig. 5. (a) Off-state I_D–V_{DS} curves and (b) electric-field distribution as a function of L_{GD} for GaN channel HEMTs with $t = 1.0$ μm and $h = 0.8$ μm. Characteristics for the HEMT with $L_{GD} = 7$ μm, $t = 2.0$ μm, and $h = 1.6$ μm are also drawn.

In order to investigate the impact of h on HEMTs with different L_{GD}, the dependence of V_{BR} on L_{GD} is shown in Fig. 5(a). L_{GD} varies from 2.5 μm to 9 μm while keeping t and h constant at 1.0 μm and 0.8 μm, respectively. The V_{BR} of the HEMT with $L_{GD} = 2.5$ μm is 582 V, which is 18 V higher than that of the same L_{GD} HEMT with $t = 0.5$ μm and $h = 0.4$ μm. The increase of V_{BR} results from the gate sidewall capacitance. For the HEMT with $L_{GD} = 2.5$ μm, the average electric-field strength at the breakdown point ($V_{DS} = 582$ V) is 2.33 MV/cm. The electric field between the gate and drain is very uniform for $V_{DS} = 550$ V as shown in Fig. 5(b). V_{BR} increases with the increase of L_{GD} for $L_{GD} \leq 5$ μm and saturates at $L_{GD} = 5$ μm. The V_{BR} for the HEMT with $L_{GD} = 5$ μm is 922 V and the electric-field distribution at $V_{DS} = 900$ V is shown in Fig. 5(b). The breakdown strength decreases from 2.33 MV/cm to 1.84 MV/cm, indicating that the gate capacitance for $t = 1.0$ μm and $h = 0.8$ μm cannot form a sufficient depletion region to make the electric field even as in the HEMT with $L_{GD} = 2.5$ μm. The electric-field curve for the HEMT with $L_{GD} = 7$ μm almost overlaps with that for the HEMT with $L_{GD} = 5$ μm for $X = 2$–7 μm ($X = 2$ μm is the starting point of L_{GD}). Thus, the gate sidewall capacitance begins to saturate when L_{GD} reaches 5 μm for $t = 1.0$ μm and $h = 0.8$ μm. In order to improve V_{BR} further, t and h are increased to 2.0 μm and 1.6 μm, respectively. V_{BR} of the HEMT with $L_{GD} = 7$ μm is increased from 953 V to 1310 V. The average breakdown strength is increased from 1.36 MV/cm to 1.87 MV/cm. For a large L_{GD}, a larger h can increase the gate sidewall capacitance more effectively, resulting in a larger depletion region and a more uniform electric-field distribution.

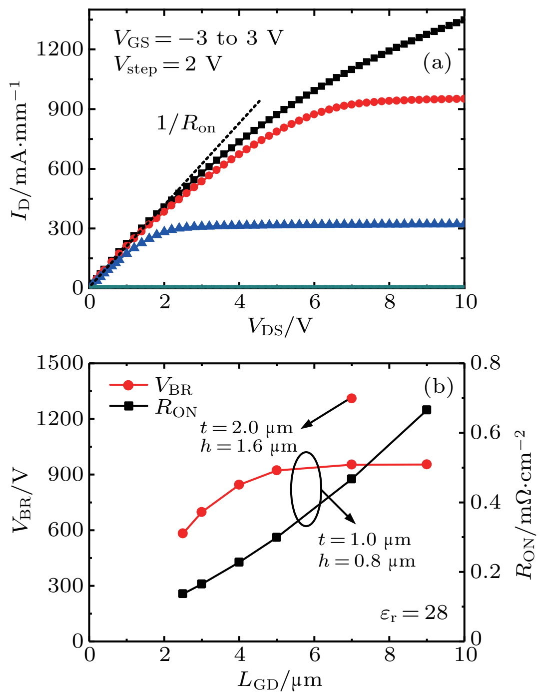

Fig. 6. (a) Output curves of the GaN channel HEMT with $L_{GD} = 7$ μm, $\varepsilon_r = 28$, $t = 2.0$ μm, and $h = 1.6$ μm. (b) V_{BR} and R_{ON} as a function of L_{GD}.

Figure 6(a) shows the output curves of the GaN channel HEMT with $L_{GD} = 7$ μm, $\varepsilon_r = 28$, $t = 2.0$ μm, and $h = 1.6$ μm. The on resistance R_{on} can be extracted from the output curves as shown in Fig. 6(a). The specific on-resistance R_{ON} is defined as $R_{ON} = R_{on} \times (L_{GS} + L_G + L_{GD} + 2L_{con})$. The dependence of V_{BR} and R_{ON} on L_{GD} is shown in Fig. 6(b). V_{BR} increases with the increase of L_{GD} for $L_{GD} \leq 5$ μm and saturates at $L_{GD} = 5$ μm. The V_{BR} is increased from 953 V to 1310 V by using a higher t and h for $L_{GD} = 7$ μm. R_{ON} increases with the increase of L_{GD}. For $L_{GD} = 2.5$ μm, $R_{ON} = 0.137$ mΩ· cm^2. The R_{ON} is increased to 0.467 mΩ· cm^2 for $L_{GD} = 7$ μm. In addition, the h values have little effect on R_{ON} for a certain L_{GD}. The power figure-of-merit (FOM) V_{BR}^2/R_{ON} is as high as 3.67×10^9 $V^2 \cdot \Omega^{-1} \cdot cm^{-2}$ for the GaN channel HEMT with $t = 2.0$ μm and $h = 1.6$ μm.

Due to the higher critical breakdown electric field, AlGaN channel HEMTs have higher breakdown voltage compared with the conventional GaN channel HEMTs. Figure 7 shows the breakdown enhancement of gate metal height for $Al_{0.7}Ga_{0.3}N/Al_{0.4}Ga_{0.6}N$ HEMTs. The breakdown voltage is increased from 1535 V to 1763 V by increasing from $t = 1.0$ μm, $h = 0.8$ μm to $t = 2.0$ μm, $h = 1.6$ μm. Due to the effect of alloy scattering in the AlGaN channel HEMT, the electron mobility would be reduced, leading to higher R_{ON} of 2.15 mΩ· cm^2 and lower FOM of 1.44×10^9 $V^2 \cdot \Omega^{-1} \cdot cm^{-2}$. The electron mobility can be improved by utilizing a buffer layer.[18] The average breakdown electric field is increased from 2.19 MV/cm to 2.51 MV/cm, which is much higher than that of GaN channel HEMTs. The potential distributions in AlGaN channel HEMTs with $t = 1.0$ μm, $h = 0.8$ μm and $t = 2.0$ μm, $h = 1.6$ μm are shown in Fig. 8. With higher gate sidewall capacitance, the potential distribution is more even and BV is enhanced. Besides the gate metal thickness, the field plate thickness could reduce the peak at the FP edge and further improve the BV. The BV enhancement mechanism of large gate metal height is similar to that of slant FP, namely, using the sidewall capacitance.[19] However, the slant FP structure requires a precise etching process to form the designed slope angle. Compared with the slant FP, the large gate metal height is more controllable. The large gate metal height would increase metal cost. In order to reduce the metal cost, metal pleating can be used instead of evaporating or sputtering process, and low cost metal can be employed instead of gold metal.

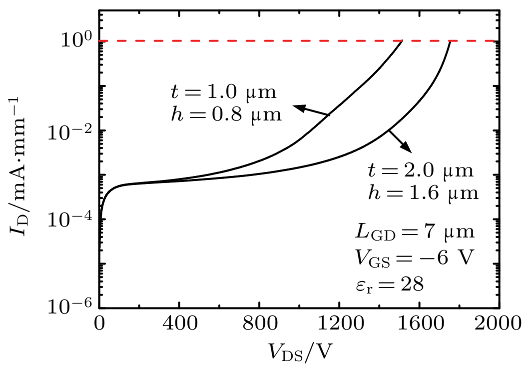

Fig. 7. Off-state I_D–V_{DS} curves of $Al_{0.7}Ga_{0.3}N/Al_{0.4}Ga_{0.6}N$ HEMTs with $h = 0.8$ μm, $t = 1.0$ μm and $h = 1.6$ μm, $t = 2.0$ μm. $L_{GD} = 7$ μm, $\varepsilon_r = 28$.

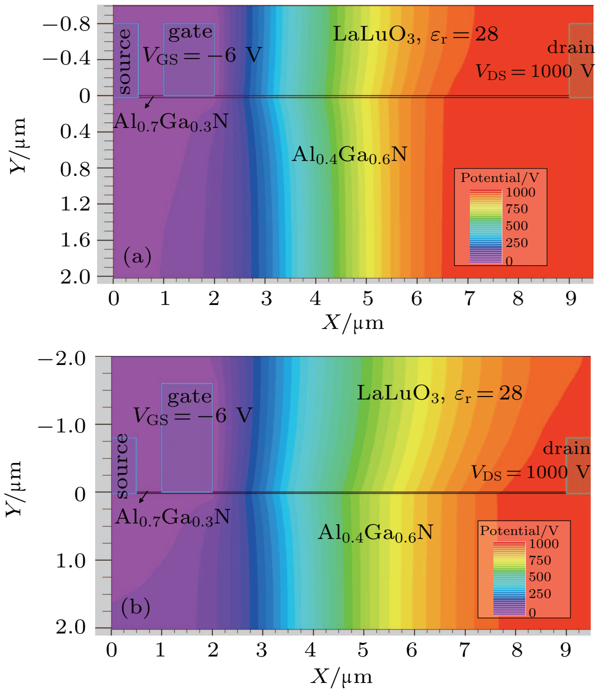

Fig. 8. Potential distribution of $Al_{0.7}Ga_{0.3}N/Al_{0.4}Ga_{0.6}N$ HEMTs with (a) $h = 0.8$ μm, $t = 1.0$ μm and (b) $h = 1.6$ μm, $t = 2.0$ μm. $L_{GD} = 7$ μm, $\varepsilon_r = 28$, and $V_{DS} = 1000$ V.

4. Conclusion

A large gate metal height is proposed to enhance BV in GaN-based HEMTs. For GaN channel HEMTs with $L_{GD} = 2.5$ μm, V_{BR} and E_{BR} are 582 V and 2.33 MV/cm, respectively by using this method. The breakdown voltage enhancement results from the increase of the gate sidewall capacitance and depletion region extension. For larger L_{GD} HEMT, larger h is essential to improve V_{BR} effectively. For the HEMT with $L_{GD} = 7$ μm, V_{BR} increases from 953 V to 1310 V by increasing h from 0.8 μm to 1.6 μm. Compared with the GaN channel HEMT, V_{BR} of the $Al_{0.4}Ga_{0.7}N$ channel HEMT is improved from 953 V to 1535 V. By increasing h from 0.8 μm to 1.6 μm, V_{BR} of the $Al_{0.4}Ga_{0.6}N$ channel HEMT is further increased from 1535 V to 1763 V. Simulation and analysis indicate that the high gate metal height is an effective method to enhance breakdown voltage in GaN-based HEMTs, and this method can be utilized in all the lateral semiconductor devices. Besides the gate metal height, a larger field plate height can be used to enhance BV with the same mechanism.

References

[1] Wu Y F, Saxler A, Moore M, Smith R P, Sheppard S, Chavarkar P M, Wisleder T, Mishra U K and Parikh P 2004 *IEEE Electron Device Lett.* **25** 117

[2] Mishra U K, Parikh P and Wu Y F 2002 *Proc. IEEE* **90** 1022

[3] Imada T, Kanamura M and Kikkawa T 2010 *Proc. IEEE Power Electron. Conf.* 1027

[4] Zhang N Q, Keller S, Parish G, Heikman S, DenBaars S P and Mishra U K 2000 *IEEE Electron Device Lett.* **21** 421

[5] Treidel E B, Hilt O, Brunner F, Würfl J and Tränkle G 2008 *IEEE Trans. Electron. Devices* **55** 3354

[6] Wang M J and Chen K J 2011 *IEEE Trans. Electron. Devices* **58** 460
[7] Lee H S, Piedra D, Sun M, Gao X, Guo S and Palacios T 2012 *IEEE Electron Device Lett.* **33** 982
[8] Nanjo T, Takeuchi M, Suita M, Oishi T, Abe Y, Tokuda Y and Aoyagi Y 2008 *Appl. Phys. Lett.* **92** 263502
[9] Nanjo T, Imai A, Suzuki Y, Abe Y, Oishi T, Suita M, Yagyu E and Aoyagi Y 2013 *IEEE Trans. Electron. Devices* **60** 1046
[10] Karmalkar S and Mishra U K 2001 *IEEE Trans. Electron. Devices* **48** 1515
[11] Xing H L, Dora Y, Chini A, Heikman S, Keller S and Mishra U K 2004 *IEEE Electron Device Lett.* **25** 161
[12] Hanawa H, Onodera H, Nakajima A and Horio K 2014 *IEEE Trans. Electron. Devices* **61** 769
[13] Ma X H, Yu H Y, Quan S, Yang L Y, Pan C Y, Yang L, Wang H, Zhang J C and Hao Y 2011 *Chin. Phys. B* **20** 027303
[14] Lian Y W, Lin Y S, Lu H C, Huang Y C and Hsu S S H 2012 *IEEE Electron Device Lett.* **33** 973
[15] Wang Y, Wang M, Xie B, Wen C P, Wang J, Hao Y, Wu W, Chen K J and Shen B 2013 *IEEE Electron Device Lett.* **34** 1370
[16] Horio K, Yonemoto K, Takayanagi H and Nakano H 2005 *J. Appl. Phys.* **98** 124502
[17] Kunihiro K, Kasahara K, Takahashi Y and Ohno Y 1999 *IEEE Electron Device Lett.* **20** 608
[18] Xiao M, Zhang J, Duan X, Zhang W, Shan H, Ning J and Hao Y 2018 *IEEE Electron Device Lett.* **39** 1149
[19] Dora Y, Chakraborty A, McCarthy L, Keller S, DenBaars S P and Mishra U K 2006 *IEEE Electron Device Lett.* **27** 713